Insecticidal Toxins from the Bacterium *Photorhabdus luminescens*

David Bowen, Thomas A. Rocheleau, Michael Blackburn, Olga Andreev, Elena Golubeva, Rohit Bhartia, Richard H. ffrench-Constant*

Transgenic plants expressing *Bacillus thuringiensis* (Bt) toxins are currently being deployed for insect control. In response to concerns about Bt resistance, we investigated a toxin secreted by a different bacterium *Photorhabdus luminescens,* which lives in the gut of entomophagous nematodes. In insects infected by the nematode, the bacteria are released into the insect hemocoel; the insect dies and the nematodes and bacteria replicate in the cadaver. The toxin consists of a series of four native complexes encoded by toxin complex loci *tca, tcb, tcc,* and *tcd*. Both *tca* and *tcd* encode complexes with high oral toxicity to *Manduca sexta* and therefore they represent potential alternatives to Bt for transgenic deployment.

Photorhabdus luminescens is a bioluminescent Gram-negative bacterium of the Enterobacteriaceae (*1*). This bacterium lives in a mutualistic association with entomophagous nematodes of the family Heterorhabditae and is released from the gut of the nematode upon invasion of the insect hemocoel by the nematode. The bacteria multiply and kill the host within 24 to 48 hours, and the nematodes feed on both the bacteria and the insect cadaver itself (*2*). At this stage, the insect host emits light produced by the bacteria. The invading nematodes reproduce within the insect and third-generation larvae then leave the cadaver in search of new hosts.

Photorhabdus luminescens can be cultured away from the host, and 50% insect mortality has been reported with fewer than five bacteria per larva (*3*). Interestingly, despite the fact that this bacterium also produces crystalline inclusion proteins (*4, 5*), a variety of antifungal and bacterial compounds (*6, 7*), and secreted proteases, lipases, and lipopolysaccharides (*2, 8–11*), our work has shown that insecticidal toxicity is associated with high molecular weight protein complexes secreted directly into the growth medium. Partially purified mixtures of these complexes are active against a wide range of insects (*12*) from several different orders (Lepidoptera, Coleoptera, and Dictyoptera), unlike different *Bacillus thuringiensis* (Bt) δ-endotoxins, which often exhibit specificity for a given insect group. In view of recent concerns about the evolution of insect resistance to transgenic crops expressing Bt (*13–15*), we are therefore investigating the use of the *Photorhabdus* toxin (Pht) as an alternative.

We purified a toxic high molecular weight protein fraction from *P. luminescens* strain W14 broth by sequential ultrafiltration, DEAE anion-exchange chromatography, and gel filtration (*16*). Subsequent high-pressure liquid chromatography (HPLC) anion-exchange chromatography revealed that this final fraction contained several peaks (Fig. 1A). Peaks A and B run as single or double complexes (A, B1/B2) on a native agarose gel (Fig. 1B) but resolve into a series of unique polypeptides (see Table 1 for NH_2-terminal sequences) with SDS–polyacrylamide gel electrophoresis (PAGE) (Fig. 1C). Complex A was responsible for most of the oral activity with smaller peaks of toxicity being associated with complexes C and D (Fig. 1D). Complex A has a median lethal dose of 875 ng per square centimeter of diet after 7 days (*17*); at doses as low as 40 ng/cm^2, larvae gained only 14% of the weight of untreated controls. CryI Bt proteins are also active against *Manduca sexta* in the nanograms per square centimeter range (*18*).

To clone the genes encoding these toxin complexes, we used monoclonal (C5F2) and polyclonal antisera against purified toxin preparations (*19*) to screen a plasmid *P. luminescens* genomic library (*20*). The antitoxin polyclonal antiserum precipitates the native toxin complexes and neutralizes oral activity against M. *sexta* (*5*). Three toxin complex–encoding loci—*tca*, *tcb*, and *tcc*—were cloned. Both *tca* and *tcc* contain three long open reading frames (ORFs) transcribed in the same direction and then a short terminal ORF in the opposite orientation (Fig. 2). The *tcb* locus consists of a single long ORF. Each ORF corresponds to one or more of the polypeptides sequenced (Table 1) from the HPLC-derived peaks (Fig. 1) except for TcaZ, TccC, and TccZ, which were not detected.

Comparison of the predicted versus the observed NH_2-terminal sequences of the different polypeptides shows that several of the polypeptides encoded by the *tc* loci are found cleaved in the bacterial supernatant. TcaA is cleaved into three polypeptides (TcaAi, TcaAii, and TcaAiii), TcaB is cleaved into two (TcaBi and TcaBii) and TcaC is apparently uncleaved. Similarly, TcbA is also cleaved into three polypeptides (TcbAi, TcbAii, and TcbAiii) whose

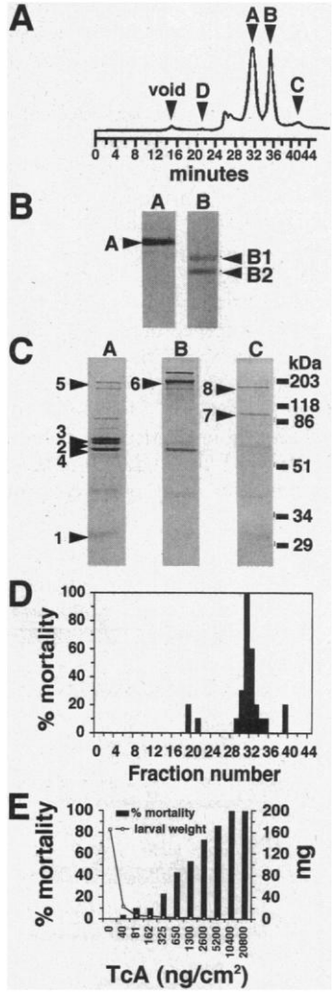

Fig. 1. Analysis of the high molecular weight toxin fraction by HPLC, native agarose gel, SDS-PAGE, and oral bioassay against *M. sexta*. (**A**) HPLC purification into four peaks: A, B, C and D. (**B**) Native gel shows HPLC peak A to be a single complex (complex A) and peak B resolves into two (B1/B2). (**C**) SDS-PAGE gel stained with Coomassie brilliant blue shows polypeptides present in each complex. Numbers indicate polypeptides with derived NH_2-terminal sequences (Table 1). (**D**) Bioassay of HPLC-derived fractions showing toxicity associated with peaks A, C, and D. (**E**) Bioassay of purified complex A showing both percentage mortality data and growth inhibition of surviving larvae (see text for discussion).

Department of Entomology, University of Wisconsin–Madison, Madison, WI 53706 USA.

*To whom correspondence should be addressed. E-mail: ffrench@vms2.macc.wisc.edu

NH_2-termini were again confirmed by sequencing (Table 1).

The *tca*, *tcb*, and *tcc* loci (GenBank accession numbers AF046867, AF047457, and AF047028) do not show overall similarity to any sequences currently deposited in GenBank. However, the predicted NH_2-terminal region of TcaC has 47% amino acid identity to the putative spvB protein, and TccA shows similarity to spvA (GenBank accession number S22664). *Salmonella* plasmid virulence (*spv*) genes are required for growth of *Salmonella dublin* in bovine macrophages (*21*). *spvB* in particular is required for *Salmonella typhimurium* to induce cytopathology in human monocyte-derived macrophages (*22*), suggesting that TcaC may attack insect hemocytes.

There is, however, considerable predicted amino acid similarity among components of Tca and Tcb. Thus, a region of 689 amino acids in TcaB (amino acids 501 to 1189) shares 40% overall identity with a 704–amino acid region of TcbA (amino acids 1801 to 2504). This identity is raised to 53% in a 151–amino acid region surrounding the proposed proteolytic cleavage sites of the two proteins (Fig. 2B). The predicted amino acid sequence of all components of Tcb shows 51.6% identity to products of a fourth locus, *tcd*—another single long ORF (Fig. 2A) (*23*), which again shares the same putative protease cleavage site (Fig. 2B). Tcd thus may be a homolog of Tcb and undergo similar proteolytic processing. *tcb* and *tcd* both encode very large proteins of a size similar to those of *Clostridium difficile* toxins A and B. Therefore, although TcbA has only a very limited overall predicted amino acid identity to these toxins (17% identity to both toxins A and B) (*24*, *25*), the similarity in the large size and processing of the toxins from both bacteria, and their effect on the gut of the host organism (*26*), may suggest similar modes of action.

To investigate the cause of oral toxicity to *M. sexta*, we used heterologous expression of the *tc* genes in *Escherichia coli* and disruption of the loci in *P. luminescens*. Although Tc proteins expressed in *E. coli* were recognized by our antibodies, they were not processed or secreted and were not orally toxic. We then deleted or disrupted each of the *tc* loci from the single *P. luminescens* strain W14, generating mutant strains tca^-, tcb^-, tcc^-, and tcd^- (Fig. 2A). Correct disruption of each of the loci was shown by Southern blot analysis and absence of the corresponding toxin complex was confirmed by Western blotting (data not shown). Deletion of either *tca* or *tcd* dramatically reduced the percentage of mortality and correspondingly increased the relative weight gain of surviving larvae (Fig. 3). Deletion of both loci in a single strain, tca^-/tcd^-, completely abolished oral toxicity. These data show that both *tca* and *tcd* loci encode orally active toxins and that,

Table 1. Characteristics of TcA, TcB, and TcC peptides (*34*).

Peptide	Kilo-daltons	NH_2-terminal sequence	
		Obtained	Predicted
1 TcaAii	25	AQDGNQDTFFSGNT	AQDGNQDTFFSGNT
2 TcaAiii	66	APLSTSELTSKLNSI	PLSTSELTSKLNSI
3 TcaBi	70	SESLFTQTLKEARR	MSESLFTQTLKEARR
4 TcaBii	60	AGGTANI-D	AGDTANIGD
5 TcaC	166	MQDSPEVSI	MQDSPEVSITT
6 TcbAii	207	FIQGYSDLFGNR	FIQGYSDLFGNR
7 TccA	105	MNQLASPLISRT	MNQLASPLISRT
8 TccB	175	MLSTMEKQLNES	MLSTMEKQLNES

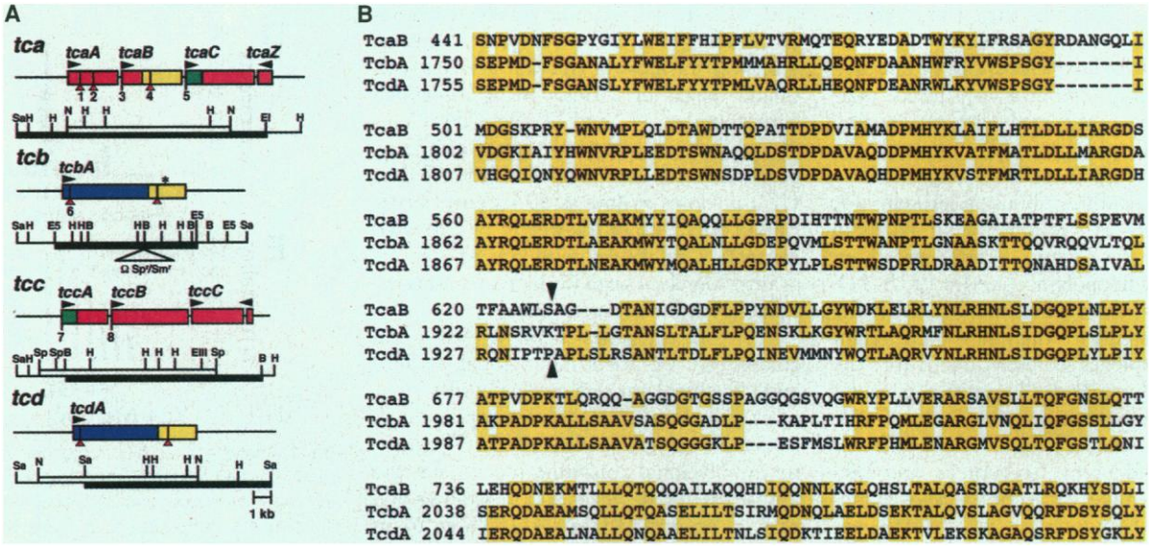

Fig. 2. (**A**) Map of the four toxin complex (*tc*)–encoding loci. *tca* and *tcc* show a similar organization with three ORFs (*tcaA, tcaB, tcaC* or *tccA, tccB, tccC*) in the same direction and a fourth (*tcaZ* or *tccZ*) transcribed in the opposite direction. NH_2-terminal sequencing of Tc proteins (numbered arrowheads) purified from growth medium (Table 1) shows that some of the encoded proteins undergo posttranslational processing. Thus, TcaA and TcaB are cleaved and TcaC appears intact. Green shading shows the regions of TcaC and TccA with similarity to the *Salmonella* virulence proteins spvB and spvA, respectively (see text). Yellow indicates regions of amino acid similarity among TcaB, TcbA, and TcdA surrounding the presumptive protease cleavage site [see (B)]. Asterisk indicates the recognition site of monoclonal antibody C5F2. Restriction maps of all Hind III sites (H) are shown below each locus, alongside other selected restriction sites used in cloning and gene disruption (B, Bgl II; EI, Eco RI; E5, Eco RV; EIII, Eco 47III; N, Ns I; Sp, Sph I; Sa, Sau 3a). Open boxes correspond to sequences deleted in knockout strains and shaded boxes correspond to restriction fragments used as probes in Southern blot analysis of the resulting mutants. (**B**) Alignment of predicted amino acid sequences from TcaB, TcbA, and TcdA showing similarity around the presumptive protease cleavage sites (arrowheads) in each.

together, they comprise the majority of activity against M. *sexta*. Interestingly, deletion of either *tcb* or *tcc* alone also reduces mortality (note the differing broth concentrations between the tc^- mutants and the wild-type W14 in Fig. 3).

The complex relationship between the toxicity of the products of all four loci in the gene knockout experiments suggests that there are interactions among the different gene products. In relation to the interaction between Tca and Tcd, several alternative hypotheses can be raised. Complex D may require complex A for enhancement of toxicity, in a fashion analogous to toxin B of C. *difficile*. Alternatively, complex D may modulate the toxicity of complex A (and possibly other complexes), as suggested by the interactions apparent in Fig. 3B. Finally, it should be noted that the above discussion is confined to oral activity against a single lepidopteran. Therefore, the apparent absence of a significant oral effect of deleting *tcb* (a clear homolog of *tcd*) and the minor effect of removing *tcc* may reflect that they are toxins active either against different groups of insects (such as Coleoptera) or by alternative routes of delivery (for example, direct introduction into the hemocoel is required for full toxicity).

To compare Pht with other toxins that are active in the gut [including the δ-endotoxins and vegetative insecticidal proteins of *B. thuringiensis* (*27–30*) and cholesterol oxidase (*31*)], we examined the histopathological effects of purified Tca (Peak A) on the gut of M. *sexta* (*32*). After M. *sexta* feed on Tca-treated diet, large cavities appear in the midgut epithelium and cellular debris appears in the gut lumen. Damage begins in the anterior of the gut and after 48 hours the disruption has spread posteriorly along the midgut, which has become totally disorganized (Fig. 4). Subsequently, the cavities in the midgut epithelium enlarge, there are no recognizable columnar cells remaining, and the lumen of the gut is packed with cell debris (Fig. 4B). Larvae then cease feeding and either die or gain little or no weight. This histopathology resembles that described for other toxins that are active in the gut (*27–30*).

In conclusion, these data show that Pht toxins are as potent as the δ-endotoxins of *B. thuringiensis* and therefore may provide useful alternatives to the deployment of Bt toxins in transgenic plants. Alternation or co-deployment of Pht and Bt toxins would prolong the effective life of both biological insecticides by delaying the evolution of resistance to either component alone. However, the interaction between the products of *tca* and *tcd* and the observed processing of the Tc polypeptides may complicate their expression in transgenic plants.

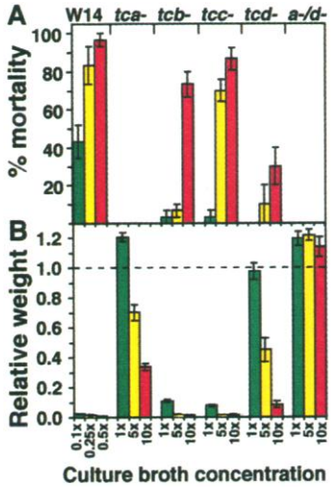

Fig. 3. Bioassay of *Manduca* neonates with the *tc* knockout strains. (**A**) Percentage mortality is shown at 1×, 5×, and 10× broth concentrations (*33*). Note that deletion of either *tca* (tca^-) or *tcd* (tcd^-) reduces toxicity and toxicity is abolished in the tca^-/tcd^- double knockout. The median effective concentrations (EC_{50}) of tca^-, tcd^-, and tca^-/tcd^- were not determinable because of low levels of toxicity (>10×). The EC_{50} and 95% confidence intervals (expressed at the broth concentration that killed 50% of larvae after 7 days) of W14 and the remaining mutants are as follows: W14, 0.11 × (0.07 to 0.17); tcb^-, 8.17 × (6.5 to 12.5); tcc^-, 4.30 × (3.2 to 5.5); tca^-/tcc^-, 8.21 × (6.0 to 14.8). (**B**) Relative weight gain of surviving larvae after 7 days of exposure to diet treated with broths from the knockout strains. Weight is expressed as a proportion of the control weight (165 + 10.5 mg; mean + SE). Note how increasing the concentration of both tca^- and tcd^- broths causes a dose-dependent reduction in growth, whereas the combination of tca^-/tcd^- in a single bacterial strain results in no weight reduction.

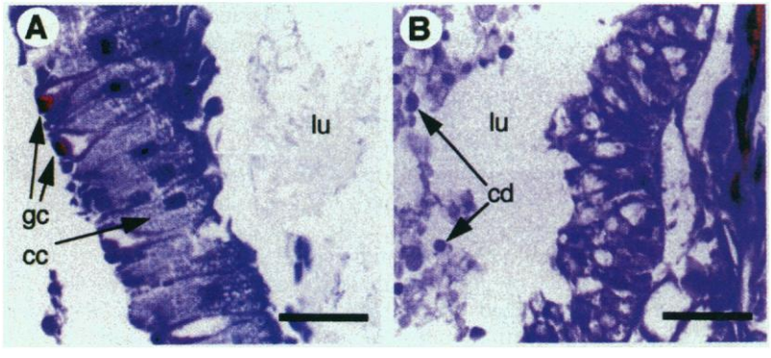

Fig. 4. Cross sections of *M. sexta* midgut epithelium either untreated (**A**) or treated (**B**) with Tca toxin. (**A**) Anterior midgut epithelium of neonate larvae 48 hours after ingesting untreated diet. Note regular arrangement of goblet cells (gc) and columnar cells (cc) in the midgut epithelium and the lumen (lu) packed with diet. (**B**) A similar section 48 hours after ingesting Tca from diet dosed at 1350 ng/cm². Note the complete disorganization of, and large cavities within, the epithelium and the presence of cellular debris (cd) in the lumen. Bar = 50 μm.

REFERENCES AND NOTES

1. G. O. Poinar, G. M. Thomas, R. Hess, *Nematology* **23**, 97 (1977).
2. G. B. Dunphy and J. M. Webster, *Int. J. Parasitol.* **18**, 729 (1988).
3. P. Gotz, A. Borman, H. G. Borman, *Proc. R. Soc. London Ser. B* **211**, 330 (1981).
4. A. Khan and W. Brooks, *J. Invertebr. Pathol.* **29**, 253 (1977).
5. D. J. Bowen, thesis, University of Wisconsin–Madison (1995).
6. R. J. Akhurst, *J. Gen. Microbiol.* **128**, 3061 (1982).
7. V. J. Paul, S. Frautschy, W. Fenical, K. H. Nealson, *J. Chem. Ecol.* **7**, 589 (1981).
8. T. M. Schmidt, B. Bleakley, K. H. Nealson, *Appl. Environ. Microbiol.* **54**, 2793 (1988).
9. G. B. Dunphy and J. M. Webster, *J. Gen. Microbiol.* **134**, 1017 (1988).
10. S. Yamanaka, A. Hagiwara, Y. Nishimura, H. Tanabe, N. Ishibashi, *Arch. Microbiol.* **158**, 387 (1992).
11. D. J. Clarke and B. C. A. Dowds, *J. Invertebr. Pathol.* **66**, 149 (1995).
12. D. Bowen and J. Ensign, *Appl. Environ. Microbiol.*, in press.
13. W. H. McGaughey, *Science* **229**, 193 (1985).
14. J. Van Rie, W. H. McGaughey, D. E. Johnson, B. D. Barnett, H. Van Mellaert, *ibid.* **247**, 72 (1990).
15. W. H. McGaughey, F. Gould, W. Gelernter, *Nature Biotechnol.* **16**, 144 (1998).
16. The culture broth was separated from the cells by centrifugation and concentrated by ultrafiltration with a 100-kD molecular mass cutoff membrane. Concentrated culture broth was applied to a DEAE Sephacel column (2.5 × 40 cm) and proteins were eluted stepwise with increasing concentrations of KCl. Fractions with oral toxicity were further concentrated and then applied to a S400HR Sephacryl gel-filtration column (2.5 × 100 cm) (Pharmacia) in phosphate buffer (100 mM KPO_4, pH 6.9). Toxic fractions were concentrated, equilibrated with 10 mM tris-HCl (pH 8.6), and loaded onto a weak anion-exchange HPLC column (301VHP575) (Vydac) and eluted with a KCl gradient.
17. Oral activity of Tca (peak A) to neonate *M. sexta* was assessed by applying doses of Tca diluted in 75 μl of HPLC buffer (10 mM tris-HCl, 250 mM KCl) to 1-cm^2 cubes of artificial diet (Gypsy moth wheat germ diet; ICN Biomedical). For the range of other insects assayed (Table 1) either a mixture of the high molecular weight toxin complexes was added to the diet as for *M. sexta* or injectable activity was measured by injection of toxin in buffer directly into the insect hemocoel. For bioassay of the *tc* gene disruptions, we used the same procedure except that instead of applying the same weight of purified Tc proteins, we added the same volume of different concentrations of culture broth to the diet cubes.
18. H. Hofte and H. R. Whitely, *Microbiol. Rev.* **53**, 242 (1989).

19. Antisera were raised against the high molecular weight toxin fraction before further separation by HPLC. A rabbit polyclonal antiserum was raised against the native toxin, and a monoclonal antibody (C5F2) was derived from mice immunized with heat-denatured toxin.
20. A plasmid DNA library was constructed in Bluescript KS$^+$ (Stratagene) from size-fractionated DNA partially digested with Sau 3a and transformed into competent library efficiency XL2-Blue MRF' *E. coli* (Stratagene). The library was screened with both the monoclonal and the polyclonal antitoxin antibodies. Immunoreactive clones were restriction mapped and sequenced with Sequenase 2.0 (United States Biochemical).
21. S. J. Libby *et al.*, *Infect. Immun.* **65**, 1786 (1997).
22. D. Guiney, personal communication.
23. J. Ensign *et al.*, World Intellectual Property, Patent WO 97/17432 (1997).
24. J. L. Johnson *et al.*, *Curr. Microbiol.* **20**, 397 (1990).
25. J. C. Phelps, L. D. Lyerly, J. L. Johnson, T. D. Wilkins, *Infect. Immun.* **59**, 150 (1991).
26. Y. Banno, R. Kobayashi, K. Kono, *Rev. Infect. Dis.* **6**, 11 (1984).
27. G. R. Sutter and E. S. Raun, *J. Invertebr. Pathol.* **9**, 90 (1967).
28. R. A. Kinsinger and W. H. McGaughey, *Ann. Entomol. Soc. Am.* **72**, 787 (1979).
29. Y. Endo and J. Nishiitsutsuji-Uwo, *J. Invertebr. Pathol.* **36**, 90 (1980).
30. C.-G. Yu, M. A. Mullins, G. W. Warren, M. G. Koziel, J. J. Estruch, *Appl. Environ. Microbiol.* **63**, 532 (1997).
31. J. P. Purcell *et al.*, *Biochem. Biophys. Res. Commun.* **196**, 1406 (1993).
32. For examination of gut pathology, we fed Tca toxin to neonate *M. sexta* for 3 hours and to first-instar larvae for 48 hours. Larvae were fixed in Bouin's fluid overnight at 4°C, dehydrated, and embedded in paraffin wax; 6-μm paraffin sections were stained with Weigert's hematoxylin followed by Cason's trichome stain; then they were examined by light microscopy.
33. Cells were spun down at 10,000*g* and then supernatants were concentrated in Millipore Centrifugal filtration units (Ultrafree, Biomax-100K) or diluted with growth medium.
34. Abbreviations for the amino acid residues are as follows: A, Ala; C, Cys; D, Asp; E, Glu; F, Phe; G, Gly; H, His; I, Ile; K, Lys; L, Leu; M, Met; N, Asn; P, Pro; Q, Gln; R, Arg; S, Ser; T, Thr; V, Val; W, Trp; and Y, Tyr.
35. We thank all at Dow AgroSciences Biotechnology for their encouragement and support of this project. Supported by Hatch funds, The Applied Research and Technology Fund, and The Industrial and Economic Development Fund, all administered by the University of Wisconsin-Madison and by DowAgrosciences.

26 March 1998; accepted 26 May 1998

TECHNICAL COMMENTS

Ambiguities in Direct Dating of Rock Surfaces Using Radiocarbon Measurements

An attempt was made to date rock surfaces with accelerator mass spectrometry (AMS) radiocarbon measurements of rock varnishes or rock weathering rinds. In two case studies, samples pretreated in the laboratory of Dr. Ronald Dorn prior to AMS analysis have been found to contain significant quantities of carbon-rich materials of two distinct classes. Type I material resembles coal, whereas type II material resembles pyrolized wood charcoal fragments. In samples where these type I and type II materials were separated and AMS-radiocarbon dated, they were found to have widely differing radiocarbon ages. In these cases, the measurement of the radiocarbon age of the entire sample would yield results that are, at best, ambiguous. Neither type I nor type II materials were found in comparable samples that were independently prepared.

Since it was first developed in the early 1980s, direct dating of rock surfaces by accelerator mass spectrometry (AMS) radiocarbon analysis has become an integral tool in the fields of geomorphology and archaeology. This technique was pioneered principally by Dr. Ronald Dorn, now at Arizona State University. Results from several studies by Dorn and co-workers (*1–13*) have implied that organic material can generally be harvested from within or beneath the rock varnish layer that commonly encrusts rock surfaces in desert regions. This varnish is composed mainly of iron and manganese oxides but may also contain small amounts of organic material, thought to be composed of bacterial remains, plant detritus, or remains of lichen or algae. These studies indicated that AMS radiocarbon dates of this organic carbon could in many cases be used to provide minimum ages of the rock surface (*1–13*).

Recently, the AMS laboratory at the University of Arizona in Tucson became involved in a research project initiated by E. Malotki of Northern Arizona University aimed at trying to obtain radiocarbon dates of petroglyphs. Petroglyphs are pictures or images that have been carved, pecked, or scratched into a rock surface. These particular petroglyphs were probably created by archaic hunter-gatherer people who populated northeastern Arizona, possibly for several thousand years before about A.D. 1 (*14*). Malotki enlisted Dorn to help collect small samples of the rock and encrusting varnish from several petroglyphs located in a canyon in northeast Arizona. Dorn then took these samples to his laboratory, where the samples were chemically pretreated before they were sent to the AMS laboratory at the University of Arizona for radiocarbon analysis. This pretreatment (*8*) included treating the samples in concentrated hydrochloric acid and concentrated hydrofluoric acid. The five samples that Dorn subsequently submitted to the Arizona AMS facility were reportedly of subvarnish rock-matrix material from the weathering rind of these rocks and did not contain samples of the varnish itself. Four of these had been taken from petroglyphs and the fifth from a control rock surface that did not have a petroglyph carved into it.

When these five samples arrived at the University of Arizona AMS laboratory, visual examination of these samples revealed that two were greenish in color, whereas the other three samples had a whitish cast. This seemed unusual because all of these samples were from the Coconino Sandstone, which is a very homogeneous rock strata. Under a binocular microscope, all five of the samples were observed to contain large quantities of black particles, as much as ~15% by volume (Fig. 1). There were two types of these particles. Type I particles are blocky, sub-angular particles with conchoidal fracture. They are jet-black in color and have glossy surfaces. These type I particles have a specific gravity greater than unity, and resemble fragments of either anthracite coal or vitrinite component of bituminous coal (Fig. 2). Many of these particles are large, 200 to 600 μm across. Analysis of this type I material showed that it contains approximately 50% carbon by mass. A specimen of this material, separated from a sample pretreated by Dorn, was forwarded to an expert on identification of coal, who identified the specimen as subbituminous coal from a vitrian layer (*15*) (Table 1).

The second type of black particles (type II) generally have a specific gravity of less than unity. They exhibit one or two pronounced lineations that resemble in size, structure, and arrangement, longitudinal tracheid cells and ray parenchyma or ray tracheid cells found in wood (Figs. 1 and 3). Many of these particles also are 200 to 600 μm in length, and a few are larger than 1000 μm in length. For comparison, a photomicrograph of bristlecone pine charcoal that we pyrolized is shown (Fig. 4). Thus, type II particles appear to be charred wood.

We separated some fragments of type I and type II carbon materials from one of these petroglyph samples in order to date each type using AMS radiocarbon measurements. These results were sufficient to show that type I grains are about 28,000 years old [conventional radiocarbon age in years before present (B.P.)], whereas type II grains are about 4000 years old (Table 2). Our failure to obtain an infinite (limiting) radiocarbon age on the coal-like material was